Global Civil Aviation Emissions Estimates for 2017–2020 Using ADS-B Data

Domingos de Azevedo Quadros, F.; Snellen, M.; Sun, Junzi; Dedoussi, I.C.

DOI
10.2514/1.C036763

Publication date
2022

Document Version
Final published version

Published in
Journal of Aircraft: devoted to aeronautical science and technology

JOURNAL OF AIRCRAFT
Vol. 59, No. 6, November–December 2022

Global Civil Aviation Emissions Estimates for 2017–2020 Using ADS-B Data

Flávio D. A. Quadros,* Mirjam Snellen,† Junzi Sun,‡ and Irene C. Dedoussi§
Delft University of Technology, 2629 HS Delft, The Netherlands

https://doi.org/10.2514/1.C036763

Aviation is a growing source of atmospheric emissions impacting the Earth's climate and air quality. Comprehensive assessments of the environmental impact of this industry require up-to-date, spatially resolved, and speciated emissions inventories. We develop and evaluate the first such estimate of global emissions from aircraft operations for the years 2017–2020. Aircraft activity data, based on flights registered by networks of aircraft Automatic Dependent Surveillance–Broadcast (ADS-B) telemetry receivers, are used together with the Base of Aircraft Data (BADA) 3.15 aircraft performance model and the International Civil Aviation Organization Engine Emissions Databank to estimate spatially resolved fuel burn and emissions of CO_2, H_2O, NO_x ($NO + NO_2$), SO_x ($SO_2 + SO_4^{2-}$), CO, unburnt hydrocarbons (HC), and nonvolatile particulate matter (nvPM). We calculate that 937 Tg of CO_2 and 4.62 Tg of NO_x were emitted by aircraft in 2019, and quantify the evolution of the fleet average emission indices over time. Owing to impacts from COVID-19, we estimate a 48% lower fuel burn, resulting in 463 Tg less CO_2 and 2.29 Tg less NO_x emitted in 2020 than what would be otherwise expected. We conclude that ADS-B is a viable source of data to generate global emissions estimates in a timely and transparent manner for monitoring and assessing aviation's atmospheric impacts.

I. Introduction

ATMOSPHERIC emissions from aviation contribute to climate change [1] and to degradation of air quality, related to human health effects [2,3]. Aviation is estimated to have contributed 3.5% of global net anthropogenic effective radiative forcing in 2011 [1], and its associated increase of ground level fine particulate matter ($PM_{2.5}$) and ozone has been estimated to have led to 16,000 premature deaths globally in 2005 [4]. Such environmental impacts should be considered when evaluating the feasibility and societal benefit of new aircraft technology concepts or policy scenarios [5,6]. Assessment of both air quality and climate impacts from aviation depend on the spatial and temporal distribution of the emissions. The air quality impacts of aviation are often regarded and generally regulated as a local air quality issue [7–9], although there is growing evidence suggesting that the majority of human health impacts might result from high altitude (cruise) emissions of oxides of nitrogen (NO_x), which affect ground-level air quality at a hemispheric range [4,10–12]. The magnitude of nonlocal human health impacts from high-altitude emissions also depends on the location of emission, due to spatial variations in atmospheric circulation and background composition, as well as population densities [11,12]. Close to airports, aviation activity can also be a significant source of primary particulate matter, with recent research indicating that emission of high number of ultrafine particles can be particularly problematic [13–15]. Concerning the climate effects, it is estimated that the non-CO_2 terms—mainly NO_x and contrail cirrus formation—represent 66% of effective radiative forcing from aviation in 2018 [1], and the climate impact of those components can be strongly dependent on the altitude [16–18], geographical location [19], and instantaneous atmospheric condition at the site of emission [20–22].

Gross aviation emissions are expected to continue to increase in the foreseeable future, with fuel burn projected to increase by 2.4–3.8 times from 2015 to 2045, despite future improvements in aircraft technology and operational efficiency [23,24], posing a threat to the fulfillment of international climate goals in this century [25]. This growth varies geographically, with Asia growing at twice the rate of Europe and North America [26]. Despite the significant reduction in air traffic that started in 2020 due to the COVID-19 pandemic [27], the aviation industry expects to resume its previously forecasted growth after a few years [28]. Recognizing the challenges of more revolutionary aircraft propulsion technologies contributing meaningfully to the reduction of emissions [29], and in order to meet its aspirational goal of carbon neutral growth after 2020 and 50% reduction in carbon emissions by 2050 relative to 2005, the International Civil Aviation Organization (ICAO) is relying on a combination of emissions offset schemes and widespread adoption of sustainable aviation fuels [30,31]. As both aviation and other sectors change the intensity, location, and make-up of their emissions over the timescale of decades, the setting for air quality and climate impacts changes along with the sensitivity of impacts to each specific activity [32–34]. The evolving and interconnected nature of this problem requires continuous reanalysis of environmental impacts and up-to-date spatially resolved aviation emissions. As the emissions are often just an intermediate step in a study—being used as input to atmospheric, climate, public health, and economic models—there is usually a large time lag between emissions data and assessments of their impact [4,35,36]. Tracking progress relative to aviation's environmental goals demands methods of producing global emission inventories with short reporting delays, capability of continuous monitoring, and with transparent sourcing of data.

Bottom-up emissions estimates can be obtained by summing emissions calculated for every individual flight known to have occurred, which is a necessary complexity to establish the spatial distribution of emissions and obtain the specific contribution of each sector, country, or aircraft type. Unlike CO_2, SO_2, and H_2O, emission of NO_x, CO, hydrocarbons (HC), black carbon, and organic carbon depend not just on the type and amount of fuel burned, but also on the engine's operating conditions, requiring simulation of individual flights. Various bottom-up aviation inventories have been compiled over the years by different institutions, using slightly different data sources and methodologies, by calculating emissions for every aircraft type and flight distance or specific origin–destination pair for a

Received 2 December 2021; revision received 10 February 2022; accepted for publication 25 March 2022; published online Open Access 29 April 2022.

*Ph.D. Candidate, Aircraft Noise and Climate Effects Section, Faculty of Aerospace Engineering, Kluyverweg 1.

†Full Professor, Aircraft Noise and Climate Effects Section, Faculty of Aerospace Engineering, Kluyverweg 1.

‡Assistant Professor, Control and Simulation Section, Faculty of Aerospace Engineering, Kluyverweg 1.

§Assistant Professor, Aircraft Noise and Climate Effects Section, Faculty of Aerospace Engineering, Kluyverweg 1; i.c.dedoussi@tudelft.nl.

list of all flight movements being considered [37]. A global list of movements is usually obtained from historical flight schedule data sold by private companies that compile them from proprietary information, largely from airlines. Besides potentially missing data for some operators, these sources do not typically capture the portion of civil aviation consisting of general aviation, charter flights, and business flights. To complement these, some studies also use primary radar, air traffic control, or movement data obtained from aviation authorities or airspace control authorities. Alternatively, top-down estimates of emissions can be made from estimates of global aviation fuel production, without distinguishing between individual flights or segments of the industry [1]. Such top-down estimates have been shown to yield larger emissions than bottom-up inventories, consistent with the additional inclusion of fuel for military, charter, and general aviation [38,39]. Table S1 in the Supplemental Material (SM) presents an overview of various aviation emissions inventories and their main sources of data.

Automatic Dependent Surveillance–Broadcast (ADS-B) is a telemetry technology used in modern aircraft that automatically transmits unencrypted aircraft identification and state at time intervals ranging from less than a second to a few seconds [40]. The affordability of ADS-B receivers enables monitoring of air traffic by individuals and has led to the creation of online networks of receivers serving data to both commercial and free online services. Modernization of air traffic control is leading its use to become mandatory for commercial aviation and other flights under instrumented flight rules in various parts of the world [41–43]. The growing availability of telemetry data recorded by ADS-B trackers has motivated their use in estimating aircraft emissions for subsets of regions, aircraft types, or chemical species. Liu et al. used such a dataset of flight movements to estimate global CO_2 emissions from aviation by considering a constant value of emissions per kilometer flown, based on a previous bottom-up estimate using flight schedule data [44]. Aircraft position data reported through ADS-B have also been used to provide actually flown trajectories to a flight model to estimate emissions [45–48]. Studies incorporating trajectories recorded by ADS-B have so far been limited to estimating emissions for specific sets of flights for which there is complete tracker coverage, unlike previous inventories based on flight schedule data, which cover all regions of the world. Additionally, ADS-B data have also been used to derive aircraft properties, generating a flight performance model independent of manufacturer-supplied data, which can then be used to estimate emissions for arbitrary flight paths [49].

In this paper, we present bottom-up estimates of global civil aviation emissions using three sources of flight movements: schedule data for the year 2018 from a market intelligence company (OAG), and activity data derived from ADS-B for the period 2017–2020 both from a commercial service (Flightradar24, data starting on July 2017) and from a noncommercial crowd-sourced platform (OpenSky). An open-source module named openAVEM is developed to calculate full-flight emissions including non-CO_2 components and allocate them into a 3-D grid for every month analyzed. Through the comparison of the resulting emissions, we establish the viability of this method to generate a comprehensive global spatially resolved inventory of civil aviation emissions, using more openly available and traceable data. Changes in emission totals and their spatial distribution over time are discussed in the context of technological improvements and inherent technological tradeoffs in aircraft engine design, and with regard to the resulting air quality and climate change impacts. This is the first study, to the authors' best knowledge, to produce spatially resolved global estimates of aviation emissions based on ADS-B data, and the first to provide an openly available, spatially resolved, and recent inventory of aviation fuel burn, CO_2, and other emissions (commonly referred to as "non-CO_2" emissions), which are the drivers of aviation's atmospheric impacts [6]. In addition, we report, for the first time, the implications of ICAO's new nonvolatile particulate matter (nvPM) measurement data for global aircraft emissions estimates for both landing and takeoff (LTO) and non-LTO portions of flights. Finally, this model is used to provide the first comprehensive, bottom-up, global emissions quantification of the COVID-19 pandemic restrictions for the aviation sector in 2020. The resulting datasets are made openly available, as described in the Appendix.

II. Methodology

The framework for creating a bottom-up aviation emissions inventory is largely similar to the approach used by the Aviation Emissions Inventory Code (AEIC) described by Simone et al. [50], as well as other such bottom-up models [37–39,51–54]. The software module developed in this study to calculate emissions (named "Open Aviation Emissions Model" or, in short, openAVEM) is tasked with lists of flights defined by origin–destination pairs for each aircraft type, sourced either from ADS-B or flight schedule data. Input data containing relevant parameters for each airport, aircraft, and engine are loaded into openAVEM, which then simulates each flight. Landing and takeoff (LTO) are modeled by a time-in-mode approach, in which emissions are proportional to the estimated time spent in each aircraft mode of operation, whereas the non-LTO portion is simulated using an aircraft performance model. From the engine's properties and the thrust, fuel burn, and ambient conditions along each flight, emissions of pollutants are calculated. Finally, the emissions of all flights are summed into a 3-D grid with a resolution of 0.5° latitude × 0.625° longitude × 500 ft altitude. Additionally, the sensitivity of results to changes in various model input parameters is considered by running openAVEM with different configurations.

A. Origin–Destination Pairs

The list of flights for which emissions are calculated is obtained from three different sources described in this section. For all three sources of flight data, flights are aggregated into a count of monthly flights for each aircraft-type–origin–destination combination.

First, 2018 historic schedule data from OAG are used, consisting of both passenger and cargo scheduled flights based largely on data provided by airlines. Global passenger service data are comprehensive, but three of the largest cargo companies are not included in this dataset: FedEx, UPS, and some of the airlines owned by DHL. A list of individual flights is built from the schedule data, which are condensed by removing duplicate entries due to code-sharing agreements, and multileg flights are separated into individual segments. The two other sources of flight movement used consist of two sets of ADS-B telemetry data: one provided by Flightradar24 (https://www.flightradar24.com), a commercial service, and another obtained from OpenSky, a nonprofit organization that manages tracker data from a collaborative network of volunteers. Data provided by Flightradar24 starts in July 2017 and extends to the end of 2020. Data obtained from OpenSky extends from the start of 2017 to the end of 2020. We note that, despite expanding in coverage over time, OpenSky still provides reduced global coverage compared with the other two sources (further discussed in Sec. D). The Flightradar24 data were prepared using the company's proprietary ADS-B and multilateration network, additional data sources, and processing procedures.

The OpenSky ADS-B data were compiled into a list of flights by Strohmeier et al. [55]. Originally in the latter dataset, flights in which the initial and final trajectories recorded ended at an altitude not higher than 2500 m had those trajectories extrapolated to ground level, and the nearest airport was assigned as the origin or destination of the flight if it lied within 10 km of the extrapolated landing. To account for emissions of flights partially recorded in the data, those conditions are relaxed: origin and destination airports are assigned to all flights regardless of the first or last altitude seen, and airports within a radius of 500 km of the extrapolated landing are considered valid for assignment (Sec. S2 of the SM). This reprocessing is done for OpenSky because we are mostly interested in the magnitude of emissions for this source of data, since its incomplete spatial coverage already precludes accurate spatial distribution at a global scale. Therefore, the main results and discussion on emissions per region of the world are focused on OAG and Flightradar24. If OpenSky coverage continues to increase over time, the need for such compromise between magnitude and spatial distribution will diminish.

Latitude and longitude coordinates and elevation for each airport given by either International Air Transport Association (IATA) or ICAO code are obtained from the OpenFlights database [56]. The number of runways and maximum runway lengths for each airport are obtained from OurAirports [57]. In the analysis of results, regional grouping of departing airports and of emissions is done according to the geoscheme used by the United Nations Statistics Division.

B. Airport, Aircraft, and Engine Data

Aircraft performance is modeled with Base of Aircraft Data (BADA) 3.15 [58]. The mapping of IATA aircraft type codes present in schedule data to ICAO type codes used by the emissions model is given in Table S2 of the SM. To exclude military flights captured in ADS-B data, which is outside the scope of this study, a list of aircraft types considered to be military is removed from the input data (Tables S3 and S4 of the SM).

Fuel mass flow rates; emission indices (EI; defined as mass emitted per mass of fuel burned) of NO_x, CO, HC, and nvPM; and additional engine information are taken primarily from certification data in the ICAO Engine Emission Databank [59]. Given that this database covers only turbofans with a rated thrust greater than 26.7 kN, it is complemented with piston engine data from the Swiss Federal Office of Civil Aviation [60], and data for older engines and some turboprops as given by the U.S. Environmental Protection Agency [61] or used by Stettler et al. [62].

Because neither ADS-B nor OAG data available to us allow the identification of specific engine models used in each individual aircraft, reference engine models are assigned to each aircraft type, according to Supplemental Tables S5–S8. This approach has been used by other global bottom-up emission inventories [39,50,53]. Additionally, to calculate emissions of narrowbody and widebody aircraft with multiple engine suppliers, we assign one model for each engine family and calculate emissions for all flights using each of those engines. The resulting emissions are then combined in a weighted sum using the aircraft-type-specific market share of each engine manufacturer (Supplemental Table S5). Within an engine family for an aircraft, there are typically multiple versions due to variants with different rated thrusts and to different design revisions. In general, the newest engine versions available are used for modeling, on the assumption that the survival rate of newer versions of each aircraft type will be higher than older versions, and that old engines might be retired to comply with tightening emissions regulations. The uncertainty in global emission estimates due to the lack of knowledge of the prevalence of specific engine versions is discussed further in Sec. III.B and in Sec. S8.3 of the SM.

C. Flight Model

The landing and takeoff portion of flights are modeled using a time-in-mode approach, in which engines are considered to run at a constant thrust for a given period of time for every phase of LTO. LTO cycles are separated into the phases of taxi-out, taxi-out acceleration, hold, takeoff, initial climb, climbout, approach, landing, reverse thrust, taxi-in acceleration, and taxi-in, according to the model proposed by Stettler et al. [62], which is based on studies conducted in the United Kingdom on airports of various sizes [63]. The use of this model instead of the simpler four-phase cycle adopted by ICAO's standard on engine emissions [64] has the intention of better capturing more modern LTO conditions, considering that the cycle suggested by ICAO remains unchanged since the first edition of the standard in 1981.

Auxiliary Power Unit (APU) emissions are modeled with times-in-mode and emission indices by aircraft class according to the "advanced approach" defined in ICAO's Airport Air Quality Manual [65]. Where data are available, the generic emission indices are substituted by known model-specific values [66]. The assignment of APU models to aircraft types is listed in Supplemental Table S9.

The climb, cruise, and descent portion of flights are simulated using the BADA 3 model following a geodesic starting from 3000 ft above the origin airport and ending 3000 ft above the destination airport. BADA formulates aircraft performance in terms of the total energy balance, considering the aircraft as a point of (varying) mass subjected to drag, lift, and thrust [58]. BADA includes aircraft aerodynamic coefficients, operational parameters such as a climb speed schedule, and other properties necessary to obtain fuel mass flow rates for different flying conditions. Wind speed is applied through all non-LTO phases using year-specific monthly average wind vectors from the MERRA-2 reanalysis product in their native $0.5° \times 0.625°$ grid with 72 hybrid-eta vertical levels [67]. Performance during each flight is affected by the wind pushing the aircraft one direction or another, but the geodesic flight trajectory is maintained. No optimization of the flight path is made by considering the wind.

Climb is simulated in steps of 1000 ft until cruise altitude, which, for flights of at least 200 NM in length, is set for each aircraft type from the most common cruise altitude observed in the first 70 days of 2020 by Flightradar24. Values of 7000 ft below the type's maximum operating altitude are adopted in case of insufficient ADS-B data (Sec. S6 of the SM). The cruise altitude for shorter flights is limited to maximum values taken as the average cruise flight level at 50–100, 100–150, and 150–200 NM flight length brackets for either turbojets or turboprops reported by Kim et al. based on aggregated radar data over North America [68]. Cruise is simulated at constant altitude in ground track steps of 50 NM. Descent is simulated in steps of 1000 ft.

D. Fuel Burn and Emissions Model

For each aircraft-type–origin–destination combination, the LTO and non-LTO phases of flight are simulated, resulting in flight segments with an associated fuel flow rate and duration. During LTO, fuel flow rate at a given thrust is piecewise linearly interpolated from available engine data. In the non-LTO phases of flight, fuel flow is precalculated in BADA as a function of thrust and speed, such that the energy and mass balance are kept while the aircraft (with its specific aerodynamic and kinetic properties) keeps a modeled schedule of speed and climb or descent rates [58]. Emissions of NO_x, CO, and HC are calculated for each segment using the Boeing Fuel Flow Method 2 [69] with the same additional considerations for edge cases used by Kim et al. [68]. This method establishes how to interpolate the emission indices between the thrust levels used for emissions certification (the points at which emissions are measured), and adjusts it from sea level to atmospheric conditions at altitude. NO_x emissions are expressed as NO_2 equivalent, and HC emissions are expressed as CH_4 equivalent. Nonvolatile particulate matter mass ($nvPM_m$) and number ($nvPM_N$) emission indices at the engine certification thrust levels are taken from measured data (corrected for system losses) when available in the ICAO database; otherwise they are estimated from smoke number using the FOA 4.0 method [65,70]. When smoke number data are also absent, such as for turboprop and piston engines, constant nvPM mass emission indices of 0 and 30 mg/kg are adopted for LTO and non-LTO, respectively, and nvPM particle numbers are disregarded, on the basis of the method used and values suggested by the U.S. Federal Aviation Administration's (FAA) emissions model, AEDT [71]. The lack of available data for those types of engines will therefore lead to an underestimate of nvPM emissions. For the non-LTO portion of flights, nvPM emissions are scaled using the same method adopted by AEDT [71], which is based on the work by Peck et al. [72]. Constant EIs of 3.155 kg/kg and 1.237 kg/kg are used for CO_2 and H_2O, respectively, the same values adopted by AEDT [71].

Initial aircraft mass for each flight is estimated following the method used by Eyers et al., which adds fuel for reserve, diversions, and time in a holding pattern according to a classification of short- or long-haul flight [39]. Payload mass is calculated as a fraction of maximum payload capacity on the basis of annual weight load factor statistics [73], with January and February 2020 using the 2019 factor, as described in Sec. S7 of the SM. Takeoff mass is calculated as the sum of aircraft empty mass, estimated fuel to cruise the entire flight distance, fuel reserves, and payload.

To account for the larger actual flight distance relative to the geodesic simplification, emissions for the non-LTO portion of flights are multiplied by a lateral inefficiency factor based on a trajectory analysis by

Seymour et al. of ADS-B telemetry data [53]. This scaling factor is equivalent to adding 3.87% plus 40.5 NM to the great circle distance. Considering that this correction is based solely on distance flown, it might overestimate fuel burn for cases in which longer trajectories are purposely flown to take advantage of favorable wind conditions, as longer paths could actually result in lower fuel consumption in that scenario [74]. While this factor adjusts the magnitude of emissions, it does not capture the true spread of their spatial distribution, with the added emissions being applied along the great circle line.

The sum of emissions calculated from the Flightradar24 flight movement data available for the second half of 2017 is scaled by a factor of 1.93 when estimating total emissions for that entire year. This is done on the basis of 51.6% of fuel burn calculated for 2018 occurring in the months of July through December, and the assumption that the month-by-month distribution of emissions is similar across both years.

E. Model Sensitivity, Uncertainty, and Limitations

The accuracy of the emissions inventories produced is a function of the accuracy of the underlying models used in the calculations. The aircraft performance model used, BADA, derives each aircraft's properties from manufacturer supplied data and in-flight measurements, with comparison of the resulting model's fuel flow and vertical speed with flight data being reported [75]. Emission rates of NO_x, HC, CO, $nvPM_m$, and $nvPM_N$ are based on measured data used to certify engine models [59]. Engine and airframe degradation are not considered in this study.

Results are compared both to similarly produced emissions inventories and to top-down estimates of fuel consumption. Factors that contribute to uncertainty include measurement errors and sample variability in determining engine emission indices, assumed specific engine model and version used by each individual aircraft, uncertainty in the models of estimating emissions at different thrust levels and atmospheric conditions relative to ground reference conditions, and estimation of takeoff mass for each flight.

The lateral inefficiency parameter corrects the amount of emissions for differences between the actual flown trajectory and the modeled trajectory, which adopts a constant cruise altitude for each aircraft type and horizontal trajectories that follow the shortest path between origin and destination. However, the actual spatial distribution of those emissions might be different from the geodesic trajectory used in the model. Potential effects of reduced air traffic in 2020 on cruise altitude and on lateral inefficiency are not evaluated in this study.

We quantify the sensitivity of emissions output to wind, LTO time-in-mode and thrust levels, aircraft-engine mapping, APU modeling, nvPM calculation methods, mass load factor, cruise flight level, flight simulation step size, and lateral inefficiency model by performing simulations with alternative input parameters. Sensitivity results are discussed throughout the Results section, with additional details presented in Sec. S8 of the SM. Noncommercial or unscheduled flights that do not have their telemetry captured—because of lack of transmitter, being outside tracker coverage, or because anonymity was requested to the tracking platforms—are not captured in either OAG or ADS-B dataset, and thus do not have their emissions counted. Finally, we note that emissions from tires, brakes, ground support equipment, road transport, and other airport activities are not considered in this study.

III. Results

A. Annual Fuel and Emission Masses

Using OAG flight schedule data, we find 280 Tg of fuel burn globally in 2018 (Table 1), which is 1.9% lower and 9.1% higher than the estimates by Graver et al. [54] and Seymour et al. [53], respectively, who also used schedule data from OAG for the same year. Within the analyzed period of 2017–2020, the annual sum of emissions is highest for 2019, with 297 Tg of fuel burn resulting from flights appearing in the ADS-B data from Flightradar24. The estimates of aviation CO_2 emissions using this source of ADS-B data are equivalent to 2.4–2.6% of all anthropogenic CO_2 emissions—excluding land-use change—for 2017–2019; this reduces to 1.4% for 2020, indicating the increased effect of COVID-19-related restrictions on aviation emissions compared with other sectors [76]. Calculated fuel burn in 2018 is 12.9% (OAG), 10.4% (Flightradar24), and 53.8% (OpenSky) lower than the worldwide jet kerosene consumption reported by the International Energy Agency (IEA, 2020), which consists of the sum of fuel delivered by producers and is not necessarily restricted to civil aviation. Few estimates are available of military aviation emissions, with previous studies estimating a military share of global aviation fuel burn of 18% in 1992 [78], 11% in 2002 [39], and a similar 10–15% range for the United States between 1990 and 2000 [79]. We note that the underestimate using OpenSky data is mainly driven by its more limited coverage, and will be discussed in the following sections. Fuel burn from international flights in 2018 is 14.7% (OAG) and 18.8% (Flightradar24) higher than the estimate for 2015 by Fleming and de Lépinay [23], with similar fractions of international to total (domestic plus international) fuel burn: 65.5% (OAG) and 65.9% (Flightradar24) versus 65% in Fleming and de Lépinay [23].

The horizontal and vertical distributions of average fuel burn rates in 2019 for the Flightradar24 dataset are shown in Fig. 1, and maps of each pollutant and each flight movement dataset are provided in Sec . S9 of the SM. We find that 92 and 65% of fuel burn shown in Fig. 1 occurs north of the equator and north of 30°N, respectively. Additionally, 72% of fuel burn occurs at altitudes higher than 9 km, representing the cruise portion of jet-powered flights. The regions with the highest share of global fuel burn occurring over them are Northern America (21%) and Eastern Asia (14%), with 23% of fuel burn occurring over the oceans between all continental regions (Sec. S9 of the SM).

Across all months, between 8.2 and 10.0% of fuel burn and 7.8 and 9.2% of NO_x are emitted during the LTO portion of flights, with the highest percentages occurring during 2020 (Sec. S10 of the SM). The

Table 1 Annual global fuel burn and emissions from civil aviation estimated from different sources of flight movement data

	OAG	Flightradar24				OpenSky			
Species	2018	2017[a]	2018	2019	2020	2017	2018	2019	2020
Fuel, Tg	280	277	288	297	157	130	149	171	95
CO_2, Tg	885	873	910	937	496	410	469	538	298
H_2O, Tg	347	342	357	367	194	161	184	211	117
SO_x, Gg[b]	168	166	173	178	94	78	89	102	57
NO_x, Tg[c]	4.32	4.26	4.47	4.62	2.44	2.08	2.38	2.71	1.49
HC, Gg	34.7	39.3	40.6	42.6	27.3	16.3	18.9	22.6	15.4
CO, Gg	624	721	753	814	569	168	312	370	234
$nvPM_m$, Gg	9.69	9.34	9.57	9.68	4.79	4.29	4.83	5.53	2.83
$nvPM_N$, 10^{26}	3.43	3.27	3.40	3.47	1.73	1.44	1.66	1.92	0.99

[a]Flightradar24 2017 values are scaled from results for the months of July–December.
[b]SO_x = oxides of sulfur, as mass of S, considering a fuel sulfur content of 600 ppm.
[c]NO_x = oxides of nitrogen, as mass of NO_2.

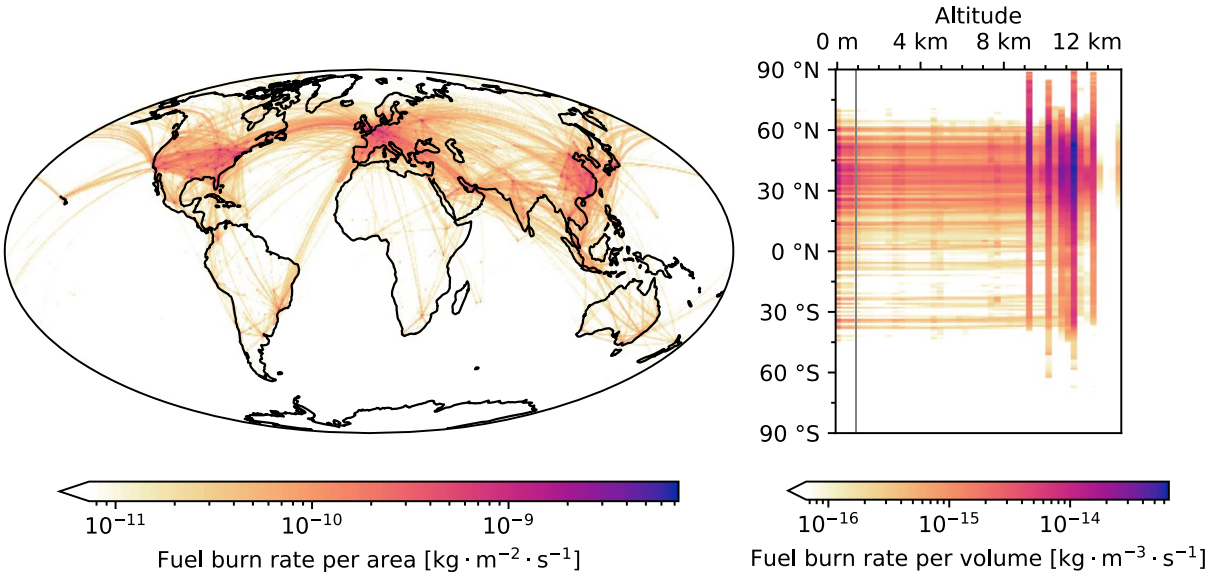

Fig. 1 Average fuel burn rates in 2019 from Flightradar24 data summed vertically (left), and averaged longitudinally (right). The thin line indicates the 3000 ft altitude (LTO threshold).

fraction of fuel burn from LTO we obtain is similar to estimates from previous studies of 8.5% for the year 2015 [6] and 9.1% for 2005 [50]. If we substitute the time-in-mode and thrust values applied here for the LTO cycle suggested by ICAO [64], the fraction of fuel burn occurring during LTO ranges from 10.8 to 13.5% (Sec. S8.2 of the SM), highlighting the uncertainty in the estimation of this portion of emissions. Considering that pushback control and reduced takeoff thrust are strategies to reduce LTO emissions that are currently being pursued [80,81], an updated model of LTO cycles could in future work be valuable in representing their emissions at a global scale. We find that although only 6.9% of fuel burn and 3.2% of NO_x emissions during LTO are due to APUs (2019 estimate using Flightradar24), APUs are responsible for 34% of $nvPM_m$ and 25% of $nvPM_N$ LTO emissions. The three alternative APU time-in-mode models evaluated lead to fuel burn between 16 and 145% higher along with a 6–8% higher average $nvPM_m$ and $nvPM_N$ EIs, while adopting different sources for the emission indices lead to between –4 and +14% $nvPM_m$ and $nvPM_N$ EIs (Sec. S8.4 of the SM). Fewer resources are openly available to estimate accurate emission indices and running times of APUs compared with aircraft main engines, but our results suggest that they are a significant contributor to low-altitude nvPM emissions.

B. Temporal Trends

Average daily fuel burn in the period between 2017 and 2020 is presented in Fig. 2, reflecting the decades-long and ongoing growth of aviation emissions, as well as the reductions due to COVID-19 restrictions. Comparing the annual fuel burn between our 2018 estimate using OAG and a 2005 inventory that also uses OAG [50], we find a globally averaged increase of 55% between the two years (Sec. S9 of the SM). This varies regionally: for example, there is a below-average increase in the fuel burned over Northern America (2%), Northern Europe (25%), and Western Europe (36%), whereas the opposite holds for Eastern Asia (131%), Southern Asia (137%), and Western Asia (177%). The spatial nonuniformity of this increase should be taken into account when assessing aviation's climate or air quality impacts, as the sensitivity of impacts can vary significantly depending on the location of emissions [11,12,19]. In addition, it further highlights the need for spatially resolved and up-to-date inventories. In terms of seasonal trends, lower and higher air traffic during boreal winter and summer, respectively, lead to fuel burn rates up to –5.7% (January) and +7.2% (August) relative to the annual averages in 2018 and 2019.

The 4.62 Tg of NO_x released by aviation globally in 2019—as estimated from the Flightradar24 dataset—represents an increase of 222 and 59% relative to values reported for 1992 [69] and 2005 [83], respectively. This is driven both by more fuel being burned and by higher emission indices: the annual global average NO_x EI of 15.5 g/kg is 3.3% higher than the value of 15.0 g/kg used by Grobler et al. [6] for the year 2015 from the AEDT inventory (Fig. 3). The observed decades-long trend of increasing NO_x EI is consistent with increases in engine overall pressure ratios and in turbine inlet

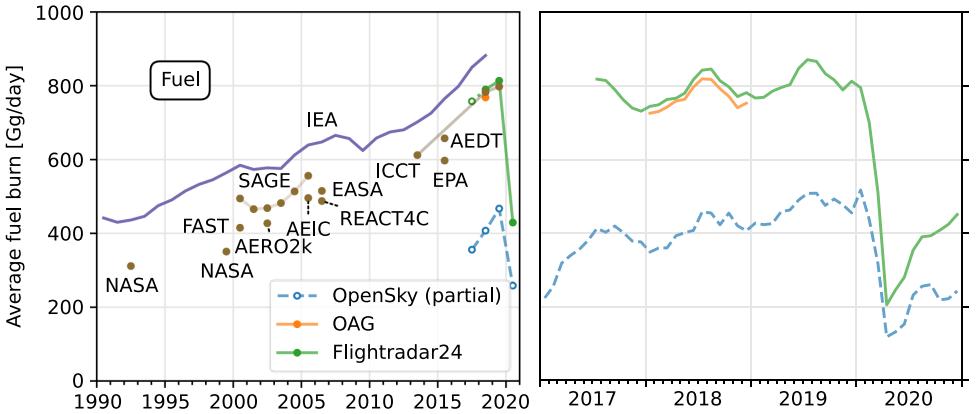

Fig. 2 Global fuel burn in the period 2017–2020 calculated from OpenSky (partial spatial coverage), OAG, and Flightradar24. Previous estimates from institutions/models[a] are also shown. ([a]The estimates from literature are shown next to the name of the institution that performed the study or name of the model used: NASA [78,82], FAST [38], AERO2k [39], SAGE [83], AEIC [50], REACT4C [35], EASA [52], ICCT [54], EPA [84], and AEDT [6,51]. The purple line represents jet kerosene consumption statistics from the IEA [77].)

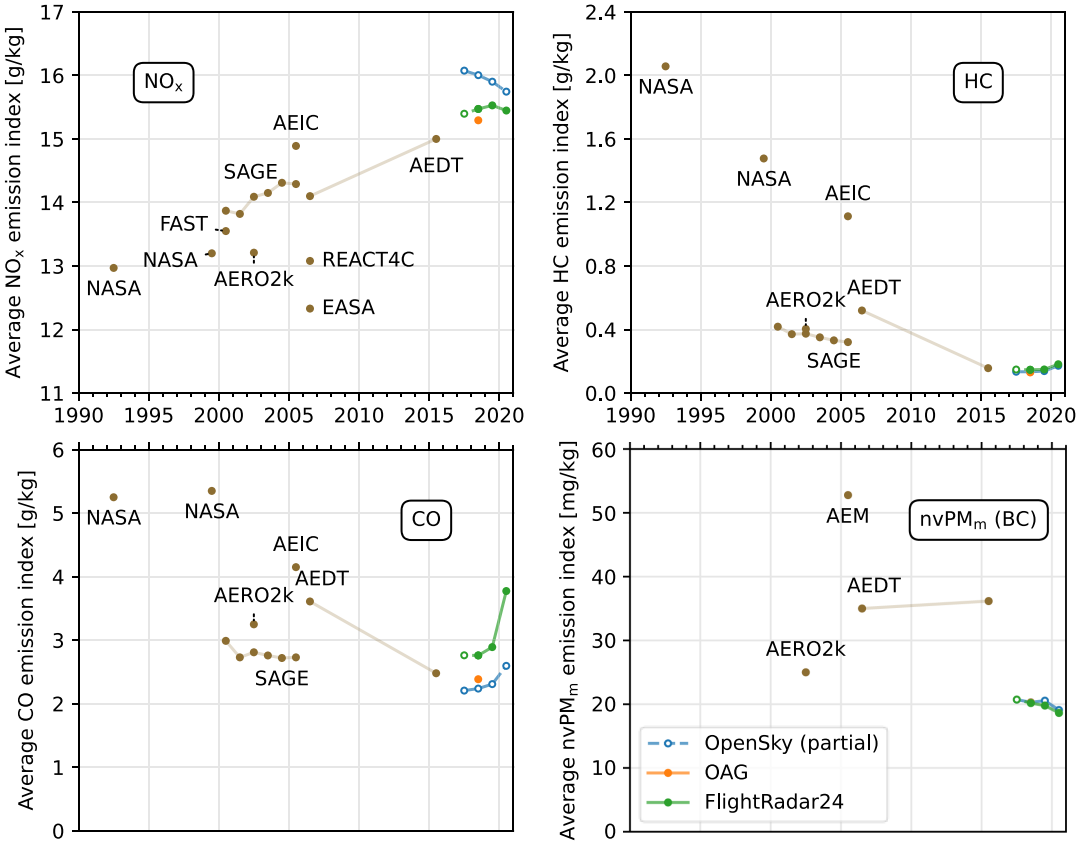

Fig. 3 Emission indices of NO_x, HC, CO, and $nvPM_m$ in the period 2017–2020 calculated: OpenSky (partial spatial coverage), OAG, and Flightradar24. Previous estimates from institutions/models[a] are also shown. ([a]Previous estimates are shown next to the name of the institution that performed the study or name of the model used: NASA [78,82], FAST [38], AERO2k [39], SAGE [83], AEIC [50], REACT4C [35], EASA [52], AEDT [6,51], and AEM [36].)

temperatures, which are pursued mainly with the goal of reducing fuel consumption [85,86]. On the other hand, higher gas temperatures, along with improved combustor designs, result in increased combustion efficiency and reduced emissions of HC and CO [3]. We find the average HC EIs for the year 2018 to be 141 mg/kg (Flightradar24) and 124 mg/kg (OAG), which are, in this order, 10 and 21% lower than the 2015 value for the AEDT inventory [6] and 73 and 76% lower compared with the AEDT inventory for 2006 [51]. The average CO EIs in 2018 of 2.61 g/kg (Flightradar24) and 2.23 g/kg (OAG) are closer to AEDT values for previous years: +5 and –10% relative to 2015 [6], and –28 and –38% relative to 2006, respectively [51]. Monthly fleet average EIs of CO and HC calculated from Flightradar24 data increased up to a maximum in June 2020 of +68 and +46%, respectively, relative to the 2019 annual averages as a consequence of the changes in traffic due to the COVID-19 pandemic (Sec. S11 of the SM).

Historically, adoption of a constant EI or the use of empirical correlations to the smoke number measurements made during engine certification have yielded a wide range of estimates of particulate matter emissions [36,87]. A standard procedure to measure nvPM EIs during engine certification was adopted in 2017 [64], with the first batch of test results being added the ICAO's Engine Emissions Databank in December 2020 [59], which we include in our model. Considering all three sources of flight movement data, we find that the global annual fleet averaged EIs for 2017–2019 for turbofan engines with certification nvPM measurements—which account for 69–75% of fuel burn given our engine aircraft assignments—are between 33.5 and 36.3 mg/kg and $1.26 \cdot 10^{15}$ and $1.38 \cdot 10^{15}$ particles/kg, and for turbofans with only smoke number data to be between 35.1 and 37.3 mg/kg and $9.03 \cdot 10^{14}$ and $1.04 \cdot 10^{15}$ particles/kg. This result, along with overall lower average EI($nvPM_m$) than previous estimates shown in Fig. 3, is consistent with the expected trend of reduced nvPM for newer engines. We also note that, by assigning a single engine to each aircraft type, we likely underrepresent older, less common, engine versions, which likely results in an underestimate of nvPM emissions.

Overall, our resulting annual nvPM EIs for 2017–2019 averaged across all aircraft types are 32.5–34.6 mg/kg and $1.11 \cdot 10^{15}$–$1.22 \cdot 10^{15}$ particles/kg. Compared with a previous estimate of 2005 emissions by Zhang et al. [36], our results are 34–39% lower in mass and 83–102% higher in particle count, driven by a combination of changes in average engine emission characteristics and methods used to calculate the emission estimates. Notably, the AEDT method employed here corrects $nvPM_m$ for altitude, but not $nvPM_N$, leading to higher particle counts in the non-LTO phases of flight [71]. Compared with estimates from Agarwal et al. [70] for 2015, our results have average nvPM EIs during LTO, excluding APUs, between 41 and 52% higher in mass and 12–15% lower in number. Using the same SCOPE11 method as Ref. [70], these differences to their 2015 LTO estimate are between 48 and 58% higher in mass and 1–4% lower in number. Our full-flight estimates are also 30–38% higher (mass) and 317–361% higher (number) than the AERO2k inventory for the year 2002 [39]. The EI($nvPM_N$) obtained here is within the range of $1 \cdot 10^{14}$ to $1 \cdot 10^{16}$ particles/kg found for typical cruise conditions by both ground [70,88,89] and in-flight measurement campaigns [90–93]. The large range of reported experimental values reflects the influence of different engine models, engine wear levels, thrust levels, atmospheric conditions, and measuring methods. Finally, our results are sensitive to the chosen nvPM estimation method. Not considering the new nvPM certification measurements and using only the FOA4 method with smoke numbers results in a 3% increase in LTO $nvPM_m$ and a 3% decrease in $nvPM_N$, the older FOA3 method leads to a 22% decrease in LTO $nvPM_m$, whereas the alternative FOX method results in $nvPM_m$ values that are 2.0 and 2.8 times our baseline for LTO and full-flight, respectively (Sec. S8.5 of the SM).

The amount of HC, CO, $nvPM_m$, $nvPM_N$, and, to a lesser extent, NO_x emissions is found be very sensitive to the choice of specific engine model and version as the reference engine in the model of each aircraft type, with outlier engine versions leading to tens of times more emissions compared to other versions (Sec. S8.3 of the SM). The effect that outliers and the uncertainty in engine allocation have

on global emissions is lessened due to the number of aircraft types contributing to the global sum of emissions, and the incorporation in our model of the contribution to emissions from each engine family in the case of aircraft that have multiple engine suppliers.

C. Reduction of Emissions in 2020

Fuel burn in the month of January increased by 3.0% between 2018 and 2019, and 3.7% between 2019 and 2020, as calculated from Flightradar24 data. That growth abruptly stopped due to the COVID-19 pandemic, with fuel burn in the month of April changing by –74.2% between 2019 and 2020. As Fig. 4 shows, the timing of the reduction in activity varied by aircraft segment. In 2019, widebodies, narrowbodies, regional jets, and business jets were responsible for 51.4, 41.9, 4.3, and 1.2% of fuel burn, respectively. During May 2020, the distribution was 67.0, 26.2, 3.4, and 1.9%, indicating that larger aircraft and business jets were less affected by the reduction in activity during this specific period. One of the possible driving factors for this is the difficulty faced in 2020 by air cargo services to meet demand with reduced passenger hold capacity available, leading to increased utilization of cargo aircraft [94].

Significant reductions in aviation emissions due to the pandemic occurred in all regions of the world in March 2020, following a decrease of 64% of fuel burn in February 2020 from flights taking off from China relative to February 2019 (Fig. 5). The proportional reduction and recovery in emissions per country varied in part due to different usual ratios of domestic and international flights, with countries that have proportionally more domestic flights, such as the United States, China, and Russia, reducing emissions less, because international routes were more impacted by pandemic-related restrictions [95]. Domestic flights were responsible for 35% of global fuel burn in the second half of 2019 and for 49% in the second half of 2020 (Sec. S12 of the SM). Overall shorter flights led to a larger share of emissions occurring during LTO: 10.0% of fuel burn, compared with 8.7% in 2019 (Sec. S10 of the SM). The changes in active fleet composition and routes flown also caused higher average EIs of HC and CO and lower average EI of nvPM during this period (Sec. S11 of the SM). Comparing the calculated global emission totals for 2020 against 2019 values scaled by +2.3%, to match the expected annual fuel consumption growth forecast by IATA in December 2019 [96], we find that actual fuel burn in 2020 was 48% lower, with 463 Tg less CO_2 and 2.29 Tg less NO_x emitted.

The changing conditions of the aviation industry in 2020 contribute to the uncertainty in estimating emissions, as the per flight deviations from the constant (annual, fleet-wide) payload mass fraction adopted are expected to be generally larger. In this period, load factors were particularly low for passenger services and particularly high for cargo services [73,94], whereas our model does not make distinctions between the two types of flight. Changing the mass load factor in our model by ±0.077 from a baseline of 0.628 leads to a

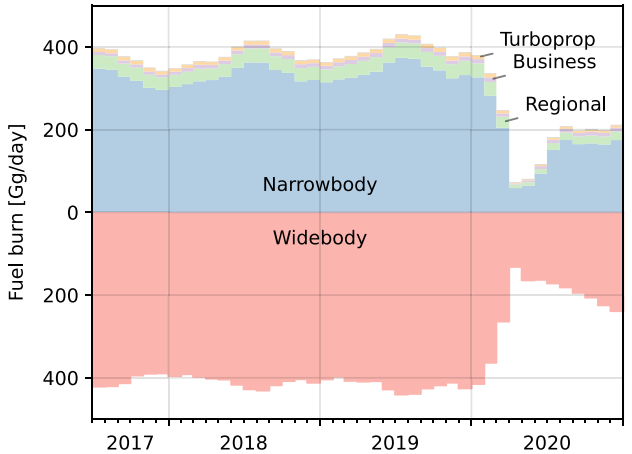

Fig. 4 Changes in monthly global civil aviation fuel burn calculated from Flightradar24 flight movement data per class of aircraft in 2017–2020.

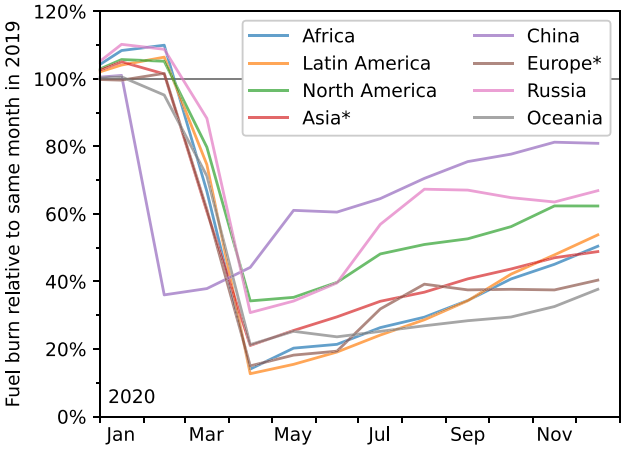

Fig. 5 Changes in monthly fuel burn calculated from Flightradar24 flight movement data per region of departure in 2020.

change of ±1.1% in global fuel burn mass (Sec. S8.6 of the SM). Lower takeoff weights and the regionally nonuniform sharp reductions in air traffic in 2020 could also bring about changes in the pattern of flown trajectories, making the cruise altitudes and lateral inefficiency correction factors adopted here (based on prepandemic data) be less representative of actual flight paths. The lateral inefficiency correction applied results in a 6.5% increase of fuel burn relative to emissions from great circle trajectories (Sec. S8.9 of the SM). This latter limitation can in future studies be overcome by using ADS-B position data to provide a more accurate estimate of lateral inefficiency during this period.

D. Viability of ADS-B and Open Data for Global Emission Estimates

Despite not all civil aircraft possessing ADS-B transmitters and tracker coverage not being globally complete, fuel burn in 2018 calculated for flights recorded by Flightradar24 is 2.8% larger than that calculated for flights in the OAG schedules (Table 1). Several factors cause differences in the two estimates of emissions, with their geographical distribution shown in Fig. 6. In regions where telemetry tracker coverage is higher—such as Europe, North America, Australia, and Japan in the case of Flightradar24—emissions estimates are higher due to unscheduled flights, including general aviation, charter, and private jet flights, which are not recorded in the data sources traditionally used to generate global emissions inventories, such as OAG. This ability to record unscheduled flights is exemplified by a previous study that demonstrated the use of an ADS-B receiver network to track a number of government- and private-operated flights [97]. The omission of the freight carriers FedEx, UPS, and DHL in the OAG data for 2018 is apparent by the large differences in fuel burn around their hubs in Memphis and Louisville. Excluding fuel from flights of these operators, the global fuel burn in 2018 calculated from Flightradar24 is still 0.5% larger than the value calculated from OAG schedules. Information from OAG on the type of service of each flight allows emissions from cargo flights to be calculated separately, and complementing those with data from Flightradar24 on the missing airlines it is possible to make a more complete estimate of emissions from cargo flights than using either source: 8.1% of fuel burn and 8.2% of NO_x from global aviation in 2018 came from cargo flights (Sec. S13 of the SM).

Estimates of emissions based on flight movement data from OpenSky were generally lower than those using Flightradar24, mainly driven by more limited geographical coverage and lack of multilateration, which is needed to track aircraft without ADS-B. Annual global fuel burn masses calculated using OpenSky were 52% (2018), 57% (2019), and 60% (2020) the values calculated using Flightradar24 (Table 1). But even in regions where coverage is nearly complete and ADS-B mandates are being implemented, such as Europe and North America, fuel burn estimated from OpenSky is still typically between 60 and 80% of the values estimated from Flightradar24 (Sec. S14 of the SM). This results from, in addition

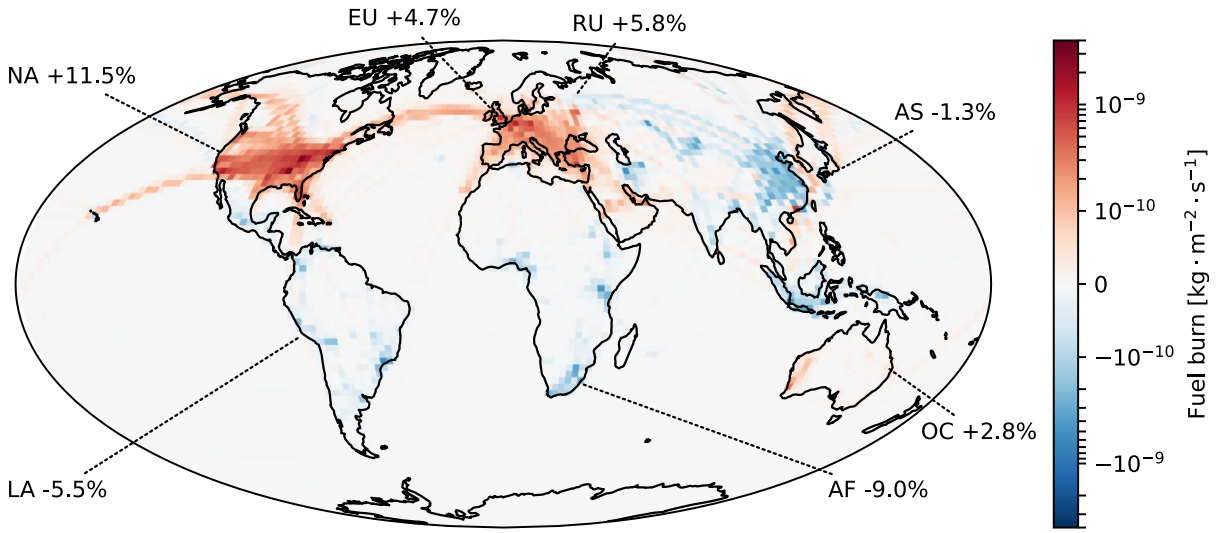

Fig. 6 Difference between fuel burn rates in 2018 from Flightradar24 ADS-B and OAG schedule data, including the relative difference in fuel burn mass from flights originating in each region.

to ADS-B tracker coverage, lack of multilateration capabilities to track aircraft without ADS-B and from absent data associating an aircraft type to each transponder's unique identifier that is transmitted. In the period of February through December 2020, between 25 and 46% of monthly flights recorded by OpenSky did not have an aircraft type assigned (Sec. S2 of the SM).

Despite these limitations, OpenSky or its underlying network of volunteer trackers could be used to estimate local or regional aviation emissions, and the open nature of this source of data also facilitates research incorporating reported aircraft positions over time to accurately represent flight trajectories [46,98]. Future research could use per flight trajectories as tracked by ADS-B directly in the flight simulation model, as opposed to considering great circle distances and assuming a lateral inefficiency factor, to improve accuracy of global emission estimates. Transparency, reproducibility, and ease of update of aviation emissions inventories could be further improved by additionally incorporating an openly available aircraft performance model derived from ADS-B [49].

IV. Conclusions

Coverage of networks like Flightradar24 and OpenSky is expected to increase due to mandates of ADS-B out capability in various airspaces and new availability of satellite receivers. We show that, already in 2018, globally more aviation emissions and 2.8% more fuel burn can be accounted for by using a network of ADS-B and multilateration trackers than by using schedule data from a market intelligence company. The different properties of flight schedule data and ADS-B data create the potential for them to be used complementarily, as exemplified by our estimate of emissions from cargo flights. The ability to include nonscheduled flights, such as military or privately operated, in emission inventories contributes to their completeness. Using this new source of data, we produce the first openly available spatially resolved 3-D inventory of global aviation emissions for the period of 2017–2020, finding that 937 Tg of CO_2, 4.62 Tg of NO_x, 42.6 Gg of hydrocarbons, 814 Gg of CO, and $3.47 \cdot 10^{26}$ nvPM with a mass of 9.68 Gg were released in 2019 directly from the operation of civil aircraft. The inventory contains only nominal values, and future work could improve on it by providing a spread of estimates based on modeling the uncertainties present in the calculation of aviation emissions.

The trend of growth in aviation emissions, demonstrated by our finding that fuel burn increased by 55% between 2005 and 2018, is expected to continue in the coming decades. And as changes in emissions from other sectors continue to change the sensitivity of local and global environmental impacts to local aviation emissions, ADS-B data can be useful in enabling more up-to-date emissions estimates, with the added benefit of increasing transparency in the calculation process. The improved agility in this method makes it easier to quantify the effects of current events on emissions, such as the 48% reduction in fuel burn in observe in 2020 relative to the fuel that was expected to be used before the COVID-19 pandemic.

For comprehensive aviation environmental impacts analyses, both CO_2 and non-CO_2 emissions are required, and more emissions reporting may be anticipated from the aviation industry in the coming years. For example, this is expected for CO_2 emissions with the adoption of market-based instruments such as ICAO's carbon offsetting scheme, called CORSIA. Scientific understanding is improving concerning aviation's non-CO_2 impacts on the climate, in part driven by NO_x emissions, but as our results indicate, the global average emission index of this pollutant is increasing over time, indicating that the growth of NO_x emissions could outpace CO_2 emissions. Because this trend is driven by engine design choices with the aim of reducing fuel consumption, inventories such as those produced here can be useful in investigating the atmospheric impacts of the tradeoff between CO_2 and NO_x emissions. This aspect of aviation's emissions will likely continue to be in focus even as the industry pledges carbon neutrality, since one of the main pathways currently being considered to achieve that goal is the adoption of sustainable aviation fuels, which is a measure that does not address NO_x emissions. In addition, the increasing awareness of the human health impacts associated with particulate matter of different sizes (including ultrafine particles, UFPs) is resulting in increased attention on these species emitted by aircraft. The combination of a spatially resolved emissions estimation tool with ADS-B data sources, such as that used in this study, can produce the required emissions data for complete and timely assessments of civil aviation's climate and air quality impacts, and contribute toward the transparent monitoring of aviation's progress toward its sustainability goals.

Appendix: Code and Gridded Emissions

The emissions inventory produced is available under the following data repository DOI: https://doi.org/10.4121/15015390 and the openAVEM code is available under DOI https://doi.org/10.4121/15062478.

Acknowledgments

Irene C. Dedoussi was supported by the Dutch Research Council (NWO Domain Applied and Engineering Sciences, Veni Project SLOPE, Project No. 18174). The authors would like to thank Flightradar24 AB and the OpenSky Network for providing Automatic Dependent Surveillance–Broadcast data, and Paul Roling for the helpful discussion on the OAG schedule data. This work was carried

out on the Dutch national e-infrastructure with the support of the SURF Cooperative. The Modern-Era Retrospective Analysis for Research and Applications, Version 2 (MERRA-2) wind data used in this study have been provided by the Global Modeling and Assimilation Office at NASA Goddard Space Flight Center.

References

[1] Lee, D. S., Fahey, D. W., Skowron, A., Allen, M. R., Burkhardt, U., Chen, Q., Doherty, S. J., Freeman, S., Forster, P. M., Fuglestvedt, J., Gettelman, A., De León, R. R., Lim, L. L., Lund, M. T., Millar, R. J., Owen, B., Penner, J. E., Pitari, G., Prather, M. J., Sausen, R., and Wilcox, L. J., "The Contribution of Global Aviation to Anthropogenic Climate Forcing for 2000 to 2018," *Atmospheric Environment*, Vol. 244, Jan. 2021, Paper 117834. https://doi.org/10.1016/j.atmosenv.2020.117834

[2] Ashok, A., Dedoussi, I. C., Yim, S. H. L., Balakrishnan, H., and Barrett, S. R. H., "Quantifying the Air Quality-CO2 Tradeoff Potential for Airports," *Atmospheric Environment*, Vol. 99, Dec. 2014, pp. 546–555. https://doi.org/10.1016/j.atmosenv.2014.10.024

[3] Masiol, M., and Harrison, R. M., "Aircraft Engine Exhaust Emissions and Other Airport-Related Contributions to Ambient Air Pollution: A Review," *Atmospheric Environment*, Vol. 95, Oct. 2014, pp. 409–455. https://doi.org/10.1016/j.atmosenv.2014.05.070

[4] Yim, S. H. L., Lee, G. L., Lee, I. H., Allroggen, F., Ashok, A., Caiazzo, F., Eastham, S. D., Malina, R., and Barrett, S. R. H., "Global, Regional and Local Health Impacts of Civil Aviation Emissions," *Environmental Research Letters*, Vol. 10, No. 3, 2015, Paper 034001. https://doi.org/10.1088/1748-9326/10/3/034001

[5] Moolchandani, K., Govindaraju, P., Roy, S., Crossley, W. A., and DeLaurentis, D. A., "Assessing Effects of Aircraft and Fuel Technology Advancement on Select Aviation Environmental Impacts," *Journal of Aircraft*, Vol. 54, No. 3, 2017, pp. 857–869. https://doi.org/10.2514/1.C033861

[6] Grobler, C., Wolfe, P. J., Dasadhikari, K., Dedoussi, I. C., Allroggen, F., Speth, R. L., Eastham, S. D., Agarwal, A., Staples, M. D., Sabnis, J., and Barrett, S. R. H., "Marginal Climate and Air Quality Costs of Aviation Emissions," *Environmental Research Letters*, Vol. 14, No. 11, 2019, Paper 114031. https://doi.org/10.1088/1748-9326/ab4942

[7] Directive (EU) 2016/2284—On the Reduction of National Emissions of Certain Atmospheric Pollutants, European Parliament and the Council of the European Union, 2016, https://data.europa.eu/eli/dir/2016/2284/oj [retrieved 8 April 2020].

[8] Airport Air Quality Manual, International Civil Aviation Organization, Montreal, 2011, Chap. 2, https://www.icao.int/publications/Documents/9889_cons_en.pdf [retrieved 19 July 2020].

[9] U.S. Environmental Protection Agency, "Control of Air Pollution from Aircraft and Aircraft Engines; Emission Standards and Test Procedures; Final Rule," *Federal Register*, Vol. 77, No. 117, 2012, pp. 36,342–36,386.

[10] Barrett, S. R. H., Britter, R. E., and Waitz, I. A., "Global Mortality Attributable to Aircraft Cruise Emissions," *Environmental Science & Technology*, Vol. 44, No. 19, 2010, pp. 7736–7742. https://doi.org/10.1021/es101325r

[11] Koo, J., Wang, Q., Henze, D. K., Waitz, I. A., and Barrett, S. R. H., "Spatial Sensitivities of Human Health Risk to Intercontinental and High-Altitude Pollution," *Atmospheric Environment*, Vol. 71, June 2013, pp. 140–147. https://doi.org/10.1016/j.atmosenv.2013.01.025

[12] Quadros, F. D. A., Snellen, M., and Dedoussi, I. C., "Regional Sensitivities of Air Quality and Human Health Impacts to Aviation Emissions," *Environmental Research Letters*, Vol. 15, No. 10, 2020, Paper 105013. https://doi.org/10.1088/1748-9326/abb2c5

[13] Keuken, M. P., Moerman, M., Zandveld, P., Henzing, J. S., and Hoek, G., "Total and Size-Resolved Particle Number and Black Carbon Concentrations in Urban Areas near Schiphol Airport (The Netherlands)," *Atmospheric Environment*, Vol. 104, March 2015, pp. 132–142. https://doi.org/10.1016/j.atmosenv.2015.01.015

[14] Jonsdottir, H. R., Delaval, M., Leni, Z., Keller, A., Brem, B. T., Siegerist, F., Schönenberger, D., Durdina, L., Elser, M., Burtscher, H., Liati, A., and Geiser, M., "Non-Volatile Particle Emissions from Aircraft Turbine Engines at Ground-Idle Induce Oxidative Stress in Bronchial Cells," *Communications Biology*, Vol. 2, No. 1, 2019, p. 90. https://doi.org/10.1038/s42003-019-0332-7

[15] Austin, E., Xiang, J., Gould, T. R., Shirai, J. H., Yun, S., Yost, M. G., Larson, T. V., and Seto, E., "Distinct Ultrafine Particle Profiles Associated with Aircraft and Roadway Traffic," *Environmental Science & Technology*, Vol. 55, No. 5, 2021, pp. 2847–2858. https://doi.org/10.1021/acs.est.0c05933

[16] Frömming, C., Ponater, M., Dahlmann, K., Grewe, V., Lee, D. S., and Sausen, R., "Aviation-Induced Radiative Forcing and Surface Temperature Change in Dependency of the Emission Altitude," *Journal of Geophysical Research: Atmospheres*, Vol. 117, No. D19, Oct. 2012, Paper D19104. https://doi.org/10.1029/2012 JD018204

[17] Matthes, S., Lim, L., Burkhardt, U., Dahlmann, K., Dietmüller, S., Grewe, V., Haslerud, A. S., Hendricks, J., Owen, B., Pitari, G., Righi, M., and Skowron, A., "Mitigation of Non-CO2 Aviation's Climate Impact by Changing Cruise Altitudes," *Aerospace*, Vol. 8, No. 2, 2021, p. 36. https://doi.org/10.3390/aerospace8020036

[18] Skowron, A., Lee, D. S., and De León, R. R., "The Assessment of the Impact of Aviation NOx on Ozone and Other Radiative Forcing Responses—The Importance of Representing Cruise Altitudes Accurately," *Atmospheric Environment*, Vol. 74, Aug. 2013, pp. 159–168. https://doi.org/10.1016/j.atmosenv.2013.03.034

[19] Skowron, A., Lee, D. S., and De León, R. R., "Variation of Radiative Forcings and Global Warming Potentials from Regional Aviation NO_x Emissions," *Atmospheric Environment*, Vol. 104, March 2015, pp. 69–78. https://doi.org/10.1016/j.atmosenv.2014.12.043

[20] Grewe, V., Dahlmann, K., Flink, J., Frömming, C., Ghosh, R., Gierens, K., Heller, R., Hendricks, J., Jöckel, P., Kaufmann, S., Kölker, K., Linke, F., Luchkova, T., Lührs, B., Van Manen, J., Matthes, S., Minikin, A., Niklaß, M., Plohr, M., Righi, M., Rosanka, S., Schmitt, A., Schumann, U., Terekhov, I., Unterstrasser, S., Vázquez-Navarro, M., Voigt, C., Wicke, K., Yamashita, H., Zahn, A., and Ziereis, H., "Mitigating the Climate Impact from Aviation: Achievements and Results of the DLR WeCare Project," *Aerospace*, Vol. 4, No. 3, 2017, p. 34. https://doi.org/10.3390/aerospace4030034

[21] Lührs, B., Linke, F., Matthes, S., Grewe, V., and Yin, F., "Climate Impact Mitigation Potential of European Air Traffic in a Weather Situation with Strong Contrail Formation," *Aerospace*, Vol. 8, No. 2, 2021, p. 50. https://doi.org/10.3390/aerospace8020050

[22] Yamashita, H., Yin, F., Grewe, V., Jöckel, P., Matthes, S., Kern, B., Dahlmann, K., and Frömming, C., "Analysis of Aircraft Routing Strategies for North Atlantic Flights by Using AirTraf 2.0," *Aerospace*, Vol. 8, No. 2, 2021, p. 33. https://doi.org/10.3390/aerospace8020033

[23] Fleming, G. G., and de Lépinay, I., "Environmental Trends in Aviation to 2050," *ICAO Environmental Report 2019: Aviation and Environment—Destination Green the Next Chapter*, International Civil Aviation Organization, Montreal, 2019, pp. 17–23.

[24] Quadros, F. D., Snellen, M., and Dedoussi, I. C., "Recent and Projected Trends in Global Civil Aviation Fleet Average NOx Emissions Indices," *AIAA Scitech 2022 Forum*, AIAA Paper 2022-2051, 2022.

[25] Grewe, V., Gangoli Rao, A., Grönstedt, T., Xisto, C., Linke, F., Melkert, J., Middel, J., Ohlenforst, B., Blakey, S., Christie, S., Matthes, S., and Dahlmann, K., "Evaluating the Climate Impact of Aviation Emission Scenarios Towards the Paris Agreement Including COVID-19 Effects," *Nature Communications*, Vol. 12, No. 1, 2021, p. 3841. https://doi.org/10.1038/s41467-021-24091-y

[26] *ICAO Long-Term Traffic Forecasts*, International Civil Aviation Organization, Montreal, 2018, https://www.icao.int/sustainability/documents/ltf_charts-results_2018edition.pdf [retrieved 25 April 2020].

[27] Dube, K., Nhamo, G., and Chikodzi, D., "COVID-19 Pandemic and Prospects for Recovery of the Global Aviation Industry," *Journal of Air Transport Management*, Vol. 92, May 2021, Paper 102022. https://doi.org/10.1016/j.jairtraman.2021.102022

[28] Commercial Market Outlook 2020-2039, Boeing Commercial Airplanes, https://www.boeing.com/cmo [retrieved 24 March 2021].

[29] Epstein, A. H., and O'Flarity, S. M., "Considerations for Reducing Aviation's CO2 with Aircraft Electric Propulsion," *Journal of Propulsion and Power*, Vol. 35, No. 3, 2019, pp. 572–582. https://doi.org/10.2514/1.B37015

[30] Resolution A40-18: Consolidated Statement of Continuing ICAO Policies and Practices Related to Environmental Protection—Climate Change, International Civil Aviation Organization, Montreal, 2019, https://www.icao.int/environmental-protection/Documents/Assembly/Resolution_A40-18_Climate_Change.pdf [retrieved 7 April 2020].

[31] ICAO Secretariat, "Introduction to the ICAO Basket of Measures to Mitigate Climate Change," *ICAO Environmental Report 2019: Aviation and Environment–Destination Green the Next Chapter*, International Civil Aviation Organization, Montreal, 2019, pp. 111–115.

[32] Silva, R. A., West, J. J., Lamarque, J.-F., Shindell, D. T., Collins, W. J., Faluvegi, G., Folberth, G. A., Horowitz, L. W., Nagashima, T., Naik, V., Rumbold, S. T., Sudo, K., Takemura, T., Bergmann, D., Cameron-Smith, P., Doherty, R. M., Josse, B., MacKenzie, I. A., Stevenson, D. S., and Zeng, G., "Future Global Mortality from Changes in Air Pollution Attributable to Climate Change," *Nature Climate Change*, Vol. 7, No. 9, 2017, pp. 647–651. https://doi.org/10.1038/nclimate3354

[33] Dedoussi, I. C., "Implications of Future Atmospheric Composition in Decision-Making for Sustainable Aviation," *Environmental Research Letters*, Vol. 16, No. 3, 2021, Paper 031002. https://doi.org/10.1088/1748-9326/abe74d

[34] Skowron, A., Lee, D. S., De León, R. R., Lim, L. L., and Owen, B., "Greater Fuel Efficiency Is Potentially Preferable to Reducing NO_x Emissions for Aviation's Climate Impacts," *Nature Communications*, Vol. 12, No. 1, 2021, p. 564. https://doi.org/10.1038/s41467-020-20771-3

[35] Søvde, O. A., Matthes, S., Skowron, A., Iachetti, D., Lim, L., Owen, B., Hodnebrog, Ø., Di Genova, G., Pitari, G., Lee, D. S., Myhre, G., and Isaksen, I. S. A., "Aircraft Emission Mitigation by Changing Route Altitude: A Multi-Model Estimate of Aircraft NOx Emission Impact on O3 Photochemistry," *Atmospheric Environment*, Vol. 95, Oct. 2014, pp. 468–479. https://doi.org/10.1016/j.atmosenv.2014.06.049

[36] Zhang, X., Chen, X., and Wang, J., "A Number-Based Inventory of Size-Resolved Black Carbon Particle Emissions by Global Civil Aviation," *Nature Communications*, Vol. 10, No. 1, 2019, p. 534. https://doi.org/10.1038/s41467-019-08491-9

[37] Olsen, S. C., Wuebbles, D. J., and Owen, B., "Comparison of Global 3-D Aviation Emissions Datasets," *Atmospheric Chemistry and Physics*, Vol. 13, No. 1, 2013, pp. 429–441. https://doi.org/10.5194/acp-13-429-2013

[38] Owen, B., Lee, D. S., and Lim, L., "Flying Into the Future: Aviation Emissions Scenarios to 2050," *Environmental Science & Technology*, Vol. 44, No. 7, 2010, pp. 2255–2260. https://doi.org/10.1021/es902530z

[39] Eyers, C. J., Norman, P., Middel, J., Plohr, M., Michot, S., Atkinson, K., and Christou, R. A., "AERO2k Global Aviation Emissions Inventories for 2002 and 2025," QinetiQ QinetiQ/04/001113, Cody Technology Park, Farnborough, England, U.K., 2004, p. 144.

[40] Sun, J., Vû, H., Ellerbroek, J., and Hoekstra, J. M., "PyModeS: Decoding Mode-S Surveillance Data for Open Air Transportation Research," *IEEE Transactions on Intelligent Transportation Systems*, Vol. 21, No. 7, July 2020, pp. 1–10. https://doi.org/10.1109/TITS.2019.2914770

[41] "Commission Implementing Regulation (EU) 2020/587 of 29 April 2020 Amending Implementing Regulation (EU) No 1206/2011 Laying down Requirements on Aircraft Identification for Surveillance for the Single European Sky and Implementing Regulation (EU) No 1207/2011 Laying down Requirements for the Performance and the Interoperability of Surveillance for the Single European Sky," Official Journal of the European Union - Legislation, 32020R0587, 2020, https://data.europa.eu/eli/reg_impl/2020/587/oj [retrieved 5 Dec. 2021].

[42] "Commission Implementing Regulation (EU) No 1207/2011 of 22 November 2011 Laying down Requirements for the Performance and the Interoperability of Surveillance for the Single European Sky," Official Journal of the European Union - Legislation, 32011R1207, 2011, https://data.europa.eu/eli/reg_impl/2011/1207/oj [retrieved 5 Dec. 2021].

[43] Title 14: Aeronautics and Space. §91.225 Automatic Dependent Surveillance-Broadcast (ADS-B) Out Equipment and Use. 14, Federal Aviation Administration. 2021.

[44] Liu, Z., Ciais, P., Deng, Z., Lei, R., Davis, S. J., Feng, S., Zheng, B., Cui, D., Dou, X., Zhu, B., Guo, R., Ke, P., Sun, T., Lu, C., He, P., Wang, Y., Yue, X., Wang, Y., Lei, Y., Zhou, H., Cai, Z., Wu, Y., Guo, R., Han, T., Xue, J., Boucher, O., Boucher, E., Chevallier, F., Tanaka, K., Wei, Y., Zhong, H., Kang, C., Zhang, N., Chen, B., Xi, F., Liu, M., Bréon, F.-M., Lu, Y., Zhang, Q., Guan, D., Gong, P., Kammen, D. M., He, K., and Schellnhuber, H. J., "Near-Real-Time Monitoring of Global CO2 Emissions Reveals the Effects of the COVID-19 Pandemic," *Nature Communications*, Vol. 11, No. 1, 2020, p. 5172. https://doi.org/10.1038/s41467-020-18922-7

[45] Filippone, A., Parkes, B., Bojdo, N., and Kelly, T., "Prediction of Aircraft Engine Emissions Using ADS-B Flight Data," *Aeronautical Journal*, Vol. 125, No. 1288, Feb. 2021, pp. 1–25. https://doi.org/10.1017/aer.2021.2

[46] Filippone, A., and Parkes, B., "Evaluation of Commuter Airplane Emissions: A European Case Study," *Transportation Research Part D: Transport and Environment*, Vol. 98, Sept. 2021, Paper 102979. https://doi.org/10.1016/j.trd.2021.102979

[47] Wang, B., Li, J., Li, C., and Wu, D., "A Method for Computing Flight Operation Fuel Burn and Emissions Based on ADS-B Trajectories," *Journal of Aeronautics, Astronautics and Aviation*, Vol. 52, No. 2, 2020, pp. 183–196. https://doi.org/10.6125/JoAAA.202006_52(2).05

[48] Sun, J., and Dedoussi, I., "Evaluation of Aviation Emissions and Environmental Costs in Europe Using OpenSky and OpenAP," *Engineering Proceedings*, Vol. 13, No. 1, 2021, p. 5. https://doi.org/10.3390/engproc2021013005

[49] Sun, J., Hoekstra, J. M., and Ellerbroek, J., "OpenAP: An Open-Source Aircraft Performance Model for Air Transportation Studies and Simulations," *Aerospace*, Vol. 7, No. 8, 2020, p. 104. https://doi.org/10.3390/aerospace7080104

[50] Simone, N. W., Stettler, M. E. J., and Barrett, S. R. H., "Rapid Estimation of Global Civil Aviation Emissions with Uncertainty Quantification," *Transportation Research Part D: Transport and Environment*, Vol. 25, Dec. 2013, pp. 33–41. https://doi.org/10.1016/j.trd.2013.07.001

[51] Wilkerson, J. T., Jacobson, M. Z., Malwitz, A., Balasubramanian, S., Wayson, R., Fleming, G., Naiman, A. D., and Lele, S. K., "Analysis of Emission Data from Global Commercial Aviation: 2004 and 2006," *Atmospheric Chemistry and Physics*, Vol. 10, No. 13, 2010, pp. 6391–6408. https://doi.org/10.5194/acp-10-6391-2010

[52] *Study on AViation and Economic Modelling (SAVE)*, European Aviation Safety Agency, MVA Consultancy, NLR, QinetiQ, and DLR, 2010, Chap. 10, https://www.easa.europa.eu/document-library/research-reports/easa2009op15 [retrieved 17 March 2021].

[53] Seymour, K., Held, M., Georges, G., and Boulouchos, K., "Fuel Estimation in Air Transportation: Modeling Global Fuel Consumption for Commercial Aviation," *Transportation Research Part D: Transport and Environment*, Vol. 88, Nov. 2020, Paper 102528. https://doi.org/10.1016/j.trd.2020.102528

[54] Graver, B., Rutherford, D., and Zheng, S., CO_2 *Emissions from Commercial Aviation: 2013, 2018, and 2019*, International Council on Clean Transportation, Washington, D.C., 2020, p. 36.

[55] Strohmeier, M., Olive, X., Lübbe, J., Schäfer, M., and Lenders, V., "Crowdsourced Air Traffic Data from the OpenSky Network 2019–2020," *Earth System Science Data*, Vol. 13, No. 2, 2021, pp. 357–366. https://doi.org/10.5194/essd-13-357-2021

[56] OpenFlights: Airport and Airline Data, https://openflights.org/data.html [retrieved 19 June 2020].

[57] Open Data @ OurAirports, https://ourairports.com/data/ [retrieved 10 Jan. 2021].

[58] Mouillet, V., *User Manual for the Base of Aircraft Data (BADA) Revision 3.15*, EUROCONTROL Experimental Centre, Brétigny-sur-Orge, France, May 2019.

[59] *ICAO Aircraft Engine Emissions Databank*, EASA, International Civil Aviation Organization, Montreal, https://www.easa.europa.eu/domains/environment/icao-aircraft-engine-emissions-databank [retrieved 13 Jan. 2021].

[60] "FOCA Aircraft Piston Engine Database," Swiss Federal Office of Civil Aviation (FOCA), https://www.bazl.admin.ch/bazl/en/home/fachleute/regulation-und-grundlagen/umwelt/schadstoffemissionen/triebwerkemissionen/zusammenfassender-bericht--anhaenge-und-datenblaetter.html [retrieved 10 May 2021].

[61] "Procedures for Emission Inventory Preparation—Volume IV: Mobile Sources," U.S. Environmental Protection Agency, Office of Air and Radiation, EPA420-R-92–009, 1992.

[62] Stettler, M. E. J., Eastham, S., and Barrett, S. R. H., "Air Quality and Public Health Impacts of UK Airports. Part I: Emissions," *Atmospheric Environment*, Vol. 45, No. 31, 2011, pp. 5415–5424. https://doi.org/10.1016/j.atmosenv.2011.07.012

[63] Watterson, J., Walker, C., and Eggleston, B., "Revision to the Method of Estimating Emissions from Aircraft in the UK Greenhouse Gas Inventory," Netcen netcen/ED47052, Abingdon, U.K., 2004.

[64] *ICAO Annex 16: Environmental Protection, Volume II–Aircraft Engine Emissions*, International Civil Aviation Organization, Montreal, 2017, https://store.icao.int/en/annex-16-environmental-protection-volume-ii-aircraft-engine-emissions [retrieved 21 April 2022].

[65] *Airport Air Quality Manual*, International Civil Aviation Organization, Montreal, 2020, https://www.icao.int/publications/pages/publication.aspx?docnum=9889 [retrieved 6 April 2020].

[66] "Expansion of Hong Kong International Airport into a Three-Runway System, Environmental Impact Assessment Report (Final)," Rept. AEIAR-185/2014, Airport Authority Hong Kong, 2014, https://www.epd.gov.hk/eia/register/report/eiareport/eia_2232014/html/index.htm [retrieved 24 April 2021].

[67] Gelaro, R., McCarty, W., Suárez, M. J., Todling, R., Molod, A., Takacs, L., Randles, C. A., Darmenov, A., Bosilovich, M. G., Reichle, R., Wargan, K., Coy, L., Cullather, R., Draper, C., Akella, S., Buchard, V., Conaty, A., da Silva, A. M., Gu, W., Kim, G.-K., Koster, R., Lucchesi, R., Merkova, D., Nielsen, J. E., Partyka, G., Pawson, S., Putman, W., Rienecker, M., Schubert, S. D., Sienkiewicz, M., and Zhao, B., "The Modern-Era Retrospective Analysis for Research and Applications, Version 2 (MERRA-2)," *Journal of Climate*, Vol. 30, No. 14, 2017, pp. 5419–5454. https://doi.org/10.1175/JCLI-D-16-0758.1

[68] Kim, B., Fleming, G., Balasubramanian, S., Malwitz, A., Lee, J., Ruggiero, J., Waitz, I., Klima, K., Stouffer, V., Long, D., Kostiuk, P., Locke, M., Holsclaw, C., Morales, A., McQueen, E., and Gillete, W., "System for Assessing Aviation's Global Emissions (SAGE), Version 1.5 Technical Manual," Federal Aviation Administration FAA-EE-2005-01, 2005, p. 234.

[69] Baughcum, S. L., Tritz, T. G., Henderson, S. C., and Pickett, D. C., "Scheduled Civil Aircraft Emission Inventories for 1992: Database Development and Analysis," NASA CR-4700, 1996, p. 205.

[70] Agarwal, A., Speth, R. L., Fritz, T. M., Jacob, S. D., Rindlisbacher, T., Iovinelli, R., Owen, B., Miake-Lye, R. C., Sabnis, J. S., and Barrett, S. R. H., "SCOPE11 Method for Estimating Aircraft Black Carbon Mass and Particle Number Emissions," *Environmental Science & Technology*, Vol. 53, No. 3, 2019, pp. 1364–1373. https://doi.org/10.1021/acs.est.8b04060

[71] "Aviation Environmental Design Tool (AEDT), Technical Manual, Version 3d," U.S. Dept. of Transportation DOT-VNTSC-FAA-21-06, 2021, p. 497.

[72] Peck, J., Oluwole, O. O., Wong, H.-W., and Miake-Lye, R. C., "An Algorithm to Estimate Aircraft Cruise Black Carbon Emissions for Use in Developing a Cruise Emissions Inventory," *Journal of the Air & Waste Management Association*, Vol. 63, No. 3, 2013, pp. 367–375. https://doi.org/10.1080/10962247.2012.751467

[73] *Airline Industry Economic Performance—April 2021—Data Tables*, International Air Transport Assoc., 2021, https://www.iata.org/en/iata-repository/publications/economic-reports/airline-industry-economic-performance---april-2021---data-tables/ [retrieved 5 April 2021].

[74] Wells, C. A., Williams, P. D., Nichols, N. K., Kalise, D., and Poll, I., "Reducing Transatlantic Flight Emissions by Fuel-Optimised Routing," *Environmental Research Letters*, Vol. 16, No. 2, 2021, Paper 025002. https://doi.org/10.1088/1748-9326/abce82

[75] Mouillet, V., "Model Accuracy Summary Report for the Base of Aircraft Data (BADA) Revision 3.15," EUROCONTROL Experimental Centre, EEC Technical/Scientific Rept. 19/03/18-48, Brétigny-sur-Orge, France, May 2019.

[76] Friedlingstein, P., O'Sullivan, M., Jones, M. W., Andrew, R. M., Hauck, J., Olsen, A., Peters, G. P., Peters, W., Pongratz, J., Sitch, S., Le Quéré, C., Canadell, J. G., Ciais, P., Jackson, R. B., Alin, S., Aragão, L. E. O. C., Arneth, A., Arora, V., Bates, N. R., Becker, M., Benoit-Cattin, A., Bittig, H. C., Bopp, L., Bultan, S., Chandra, N., Chevallier, F., Chini, L. P., Evans, W., Florentie, L., Forster, P. M., Gasser, T., Gehlen, M., Gilfillan, D., Gkritzalis, T., Gregor, L., Gruber, N., Harris, I., Hartung, K., Haverd, V., Houghton, R. A., Ilyina, T., Jain, A. K., Joetzjer, E., Kadono, K., Kato, E., Kitidis, V., Korsbakken, J. I., Landschützer, P., Lefèvre, N., Lenton, A., Lienert, S., Liu, Z., Lombardozzi, D., Marland, G., Metzl, N., Munro, D. R., Nabel, J. E. M. S., Nakaoka, S.-I., Niwa, Y., O'Brien, K., Ono, T., Palmer, P. I., Pierrot, D., Poulter, B., Resplandy, L., Robertson, E., Rödenbeck, C., Schwinger, J., Séférian, R., Skjelvan, I., Smith, A. J. P., Sutton, A. J., Tanhua, T., Tans, P. P., Tian, H., Tilbrook, B., van der Werf, G., Vuichard, N., Walker, A. P., Wanninkhof, R., Watson, A. J., Willis, D., Wiltshire, A. J., Yuan, W., Yue, X., and Zaehle, S., "Global Carbon Budget 2020," *Earth System Science Data*, Vol. 12, No. 4, 2020, pp. 3269–3340. https://doi.org/10.5194/essd-12-3269-2020

[77] *Oil Information 2020*, International Energy Agency, 2020, https://www.iea.org/data-and-statistics/data-browser?country=WORLD&fuel=Oil&indicator=OilProductsCons [retrieved 11 May 2021].

[78] Mortlock, A., and Van Alstyne, R., "Military, Charter, Unreported Domestic Traffic and General Aviation 1976, 1984, 1992, and 2015 Emission Scenarios," NASA CR-1998-207639, 1998, p. 120.

[79] Waitz, I. A., Lukachko, S. P., and Lee, J. J., "Military Aviation and the Environment: Historical Trends and Comparison to Civil Aviation," *Journal of Aircraft*, Vol. 42, No. 2, 2005, pp. 329–339. https://doi.org/10.2514/1.6888

[80] Ashok, A., Balakrishnan, H., and Barrett, S. R. H., "Reducing the Air Quality and CO2 Climate Impacts of Taxi and Takeoff Operations at Airports," *Transportation Research Part D: Transport and Environment*, Vol. 54, July 2017, pp. 287–303. https://doi.org/10.1016/j.trd.2017.05.013

[81] Koudis, G. S., Hu, S. J., Majumdar, A., Jones, R., and Stettler, M. E. J., "Airport Emissions Reductions from Reduced Thrust Takeoff Operations," *Transportation Research Part D: Transport and Environment*, Vol. 52, May 2017, pp. 15–28. https://doi.org/10.1016/j.trd.2017.02.004

[82] Sutkus, D. J., Baughcum, S. L., and DuBois, D. P., "Scheduled Civil Aircraft Emission Inventories for 1999: Database Development and Analysis," NASA CR-2001-211216, 2001, p. 131.

[83] Kim, B. Y., Fleming, G. G., Lee, J. J., Waitz, I. A., Clarke, J.-P., Balasubramanian, S., Malwitz, A., Klima, K., Locke, M., Holsclaw, C. A., Maurice, L. Q., and Gupta, M. L., "System for Assessing Aviation's Global Emissions (SAGE), Part 1: Model Description and Inventory Results," *Transportation Research Part D: Transport and Environment*, Vol. 12, No. 5, 2007, pp. 325–346. https://doi.org/10.1016/j.trd.2007.03.007

[84] "EPA Technical Report on Aircraft Emissions Inventory and Stringency Analysis," U.S. Environmental Protection Agency, Washington, D.C., 2020, https://cfpub.epa.gov/si/si_public_record_report.cfm?Lab=OTAQ&dirEntryID=343254 [retrieved 16 March 2021].

[85] Kyprianidis, K. G., and Dahlquist, E., "On the Trade-Off Between Aviation NOx and Energy Efficiency," *Applied Energy*, Vol. 185, Jan. 2017, pp. 1506–1516. https://doi.org/10.1016/j.apenergy.2015.12.055

[86] Freeman, S., Lee, D. S., Lim, L. L., Skowron, A., and De León, R. R., "Trading off Aircraft Fuel Burn and NO_x Emissions for Optimal Climate Policy," *Environmental Science & Technology*, Vol. 52, No. 5, 2018, pp. 2498–2505. https://doi.org/10.1021/acs.est.7b05719

[87] Abrahamson, J. P., Zelina, J., Andac, M. G., and Vander Wal, R. L., "Predictive Model Development for Aviation Black Carbon Mass Emissions from Alternative and Conventional Fuels at Ground and Cruise," *Environmental Science & Technology*, Vol. 50, No. 21, 2016, pp. 12,048–12,055. https://doi.org/10.1021/acs.est.6b03749

[88] Durdina, L., Brem, B. T., Elser, M., Schönenberger, D., Siegerist, F., and Anet, J. G., "Reduction of Nonvolatile Particulate Matter Emissions of a Commercial Turbofan Engine at the Ground Level from the Use of a Sustainable Aviation Fuel Blend," *Environmental Science & Technology*, Vol. 55, No. 21, 2021, pp. 14,576–14,585. https://doi.org/10.1021/acs.est.1c04744

[89] Lobo, P., Durdina, L., Smallwood, G. J., Rindlisbacher, T., Siegerist, F., Black, E. A., Yu, Z., Mensah, A. A., Hagen, D. E., Miake-Lye, R. C., Thomson, K. A., Brem, B. T., Corbin, J. C., Abegglen, M., Sierau, B., Whitefield, P. D., and Wang, J., "Measurement of Aircraft Engine Non-Volatile PM Emissions: Results of the Aviation-Particle Regulatory Instrumentation Demonstration Experiment (A-PRIDE) 4 Campaign," *Aerosol Science and Technology*, Vol. 49, No. 7, 2015, pp. 472–484. https://doi.org/10.1080/02786826.2015.1047012

[90] Moore, R. H., Thornhill, K. L., Weinzierl, B., Sauer, D., D'Ascoli, E., Kim, J., Lichtenstern, M., Scheibe, M., Beaton, B., Beyersdorf, A. J., Barrick, J., Bulzan, D., Corr, C. A., Crosbie, E., Jurkat, T., Martin, R., Riddick, D., Shook, M., Slover, G., Voigt, C., White, R., Winstead, E., Yasky, R., Ziemba, L. D., Brown, A., Schlager, H., and Anderson, B. E., "Biofuel Blending Reduces Particle Emissions from Aircraft Engines at Cruise Conditions," *Nature*, Vol. 543, No. 7645, 2017, pp. 411–415. https://doi.org/10.1038/nature21420

[91] Moore, R. H., Shook, M., Beyersdorf, A., Corr, C., Herndon, S., Knighton, W. B., Miake-Lye, R., Thornhill, K. L., Winstead, E. L., Yu, Z., Ziemba, L. D., and Anderson, B. E., "Influence of Jet Fuel Composition on Aircraft Engine Emissions: A Synthesis of Aerosol Emissions Data from the NASA APEX, AAFEX, and ACCESS Missions," *Energy & Fuels*, Vol. 29, No. 4, 2015, pp. 2591–2600. https://doi.org/10.1021/ef502618w

[92] Schripp, T., Anderson, B., Crosbie, E. C., Moore, R. H., Herrmann, F., Oßwald, P., Wahl, C., Kapernaum, M., Köhler, M., Le Clercq, P., Rauch, B., Eichler, P., Mikoviny, T., and Wisthaler, A., "Impact of Alternative Jet Fuels on Engine Exhaust Composition During the 2015 ECLIF Ground-Based Measurements Campaign," *Environmental Science & Technology*, Vol. 52, No. 8, 2018, pp. 4969–4978. https://doi.org/10.1021/acs.est.7b06244

[93] Voigt, C., Kleine, J., Sauer, D., Moore, R. H., Bräuer, T., Le Clercq, P., Kaufmann, S., Scheibe, M., Jurkat-Witschas, T., Aigner, M., Bauder, U., Boose, Y., Borrmann, S., Crosbie, E., Diskin, G. S., DiGangi, J., Hahn, V., Heckl, C., Huber, F., Nowak, J. B., Rapp, M., Rauch, B., Robinson, C., Schripp, T., Shook, M., Winstead, E., Ziemba, L., Schlager, H., and Anderson, B. E., "Cleaner Burning Aviation Fuels Can Reduce Contrail Cloudiness," *Communications Earth & Environment*, Vol. 2, No. 1, 2021, pp. 1–10. https://doi.org/10.1038/s43247-021-00174-y

[94] *Air Cargo Market Analysis*, International Air Transport Assoc., May 2021, https://www.iata.org/en/iata-repository/publications/economic-reports/air-freight-monthly-analysis---may-2021/ [retrieved 15 July 2021].

[95] *Annual Review 2020*, International Air Transport Assoc., 2019, https://www.iata.org/contentassets/c81222d96c9a4e0bb4ff6ced0126f0bb/iata-annual-review-2020.pdf [retrieved 3 Jan. 2021].

[96] "Airline Industry Economic Performance–Dec. 2019–Report," International Air Transport Assoc., 2019, https://www.iata.org/en/iata-repository/publications/economic-reports/airline-industry-economic-performance---december-2019---report/ [retrieved 6 May 2021].

[97] Strohmeier, M., Smith, M., Lenders, V., and Martinovic, I., "The Real First Class? Inferring Confidential Corporate Mergers and Government Relations from Air Traffic Communication," *2018 IEEE European Symposium on Security and Privacy (EuroS P)*, IEEE, New York, 2018, pp. 107–121.

[98] Sun, J., Hoekstra, J. M., and Ellerbroek, J., "Estimating Aircraft Drag Polar Using Open Flight Surveillance Data and a Stochastic Total Energy Model," *Transportation Research Part C: Emerging Technologies*, Vol. 114, May 2020, pp. 391–404. https://doi.org/10.1016/j.trc.2020.01.026